CONTRACTILE EVENTS IN THE CILIA OF *PARAMECIUM, OPALINA, MYTILUS,* AND *PHRAGMATOPOMA*

ROBERT RIKMENSPOEL

From the Department of Biological Sciences, State University of New York, Albany, New York 12222

ABSTRACT The motion of the abnormal cilia of *Opalina* and *Mytilus* can be described by the recently developed model for ciliary motion, provided the activation of the contractility during the effective stroke is reduced by three- to fivefold compared with that in the recovery stroke. The stiffness of the *Mytilus* cilium during the effective stroke is found several hundred times larger than that predicted by the model, however. The stiffness of the cilia of *Paramecium, Opalina, Phragmatopoma,* and of *Mytilus* in the recovery phase, is predicted approximately correctly by the model. The activation of contractility in *Mytilus* and *Phragmatopoma* cilia increases with the viscosity of the medium, as the velocity of the ciliary motion slows down. This leads to the equivalent of a force-velocity relation. The velocity of propagation of the bend in the cilia during the recovery stroke is shown to be dependent only on the elastic properties of the ciliary shaft, and to be independent of the contractile activity.

INTRODUCTION

In a recent paper a model was developed for the contractile events in cilia (Rikmenspoel and Rudd, 1973). In this model the active forces in cilia, and the stiffness of the ciliary shaft are generated from a simple prescription for the attachment and loosening of the dynein crossbridges between sliding tubulin fibers. The model was able to reproduce the shape of the ciliary stroke in a variety of cilia (*Sabellaria, Paramecium, Stentor, Jorunna, Pleurobrachia*). All these cilia have in common that a normal, water transporting, effective stroke can be clearly distinguished from a recovery stroke.

In this paper the model is applied to the abnormal forms of ciliary motion in *Opalina* and *Mytilus*. In these organisms the recovery stroke of the cilia appears to be the functional one (Sleigh, 1968; Blake and Sleigh, 1974), with the effective stroke serving to return the organelles to their original position. The behavior of the cilia of *Mytilus* and of the normal cilia of *Phragmatopoma* is investigated at raised viscosity.

Baba (1972) has recently published values for the stiffness of the *Mytilus* cilium, which are much higher than would be predicted from the model of Rikmenspoel and Rudd (1973). The simple, normal cilium of *Paramecium* represents probably the best object for verifying stiffnesses predicted by the model. Since Machemer (1972, 1974)

has presented new, accurate data on the motion of this cilium, a new analysis of *Paramecium* is presented in this paper. For all cilia treated special attention is paid to the stiffness. A preliminary publication of some of the results in this paper has been made recently (Rikmenspoel, 1974).

EXPERIMENTAL DATA

Paramecium. Still photographs of *Paramecium* have been published by Machemer (1972). In these photographs the cilia covering the body of the cells show the progression of the metachronal wave. Plate 1 of Machemer (1972), showing an organism at 1.0 cP, was rephotographed and projected onto tracing paper. The progression of the metachronal wave at a velocity of 345 μm/s, makes that the cilia are seen at different phases of the ciliary cycle. Assuming a regular progression of the metachronal wave the phase of each cilium in the projected image relative to a chosen reference point can be calculated. Tracings were made of cilia chosen such that they represented phase differences of a multiple of approximately 36° (1/10 of a cycle) from the start of the recovery stroke. By combining these tracings a complete cycle of the cilia was constructed, at time intervals of approximately 3 ms.

It would be preferable to have high speed cinemicrographs, from which tracings of a single cilium during the cycle could be made. The high magnification necessary for these small cilia, combined with their high frequency and the need for Nomarski illumination appears to preclude the taking of such cinemicrographs with present techniques, however. The photographs of *Paramecium* at raised viscosity published by Machemer (1972) did not have enough clarity and do not show a regular enough progression of the metachronal wave to make a construction of a ciliary cycle possible.

Opalina. A tracing of the cilium of *Opalina* was taken from Sleigh (1960). This tracing, shown in Fig. 4 below, was constructed by Sleigh from photographs in an analogous way to that outlined above for *Paramecium.*

Mytilus edulis was obtained from the Northeast Marine Specimens Co., Woods Hole, Mass. Gills of the mussels were excised and immersed in artificial seawater. The viscosity of the artificial seawater was raised by the addition of Ficoll to up to 330 cP.

Moving films were made using a 45X Zeiss water immersion phase objective (Carl Zeiss, Inc., New York). For analysis large solitary cilia were selected on the films that were not obstructed in any way, showed a regular motion and stayed in focus over their whole length during the cycle. Due to the large variation in length of the cilia of *Mytilus* it was not possible to find cilia of the same length for every viscosity, which fulfilled all the requirements.

Phragmatopoma,[1] an organism which closely resembles and which belongs to the same family as the more familiar *Sabellaria*, was obtained from the Pacific Bio-Marine Supply Co., Venice, Calif. Gills of the organisms were excised and suspended in artificial seawater. The viscosity of the artificial seawater was raised with Ficoll.

---

[1] I thank Dr. Stephen Brown for pointing out *Phragmatopoma* as an analogue to *Sabellaria.*

The cilia of *Phragmatopoma* are implanted in rows, as shown in Fig. 1 below. Moving films were made with the gills oriented such that the rows of cilia were along the line of sight. Nomarski differential interference optics with a 100X Zeiss oil immersion objective were used to limit the depth of focus. By this optical sectioning a single cilium of a row could be projected sharply on to the film. The direction of optical shear, in which no optical contrast is obtained, was chosen in all cases such that the cilia were not visible at the end of the effective stroke. Consequently the transition between the effective and the recovery stroke was not recorded (see Fig. 7 below).

Using Nomarski optics reduced the amount of light available to such an extent that no films at a higher rate than 200 frames/s could be taken. This proved unsatisfactorily slow for cilia at normal viscosity (1.4 cP) and no data at 1.4 cP are reported. When the cilia were slowed down by raising the viscosity, good tracings could be made from the films at viscosities of 2.1 cP and higher.

Moving films were made at 200 frames/s with a Millikan DBM-5C camera (Teledyne Corp., Arcadia, Calif.) as described before (Eykhout and Rikmenspoel, 1960). Tracings of the ciliary positions were made with the aid of a Vanguard C-11 motion analyzer (Vanguard Instrument Corp., Melville, N.Y.).

For scanning electron microscopy gills of *Phragmatopoma* were fixed and dehydrated according to Karnovsky (1965). After critical point drying, the specimen were mounted on studs with double-faced Scotch tape, and gold coated. Scanning electron micrographs were made on a Stereo-scan Mark II (Cambridge Instrument Co., London SW1).

Ficoll was obtained from Sigma Chemical Co., St. Louis, Mo. Solutions of Ficoll were made up fresh for each experiment. The viscosity of the artificial seawater-Ficoll solutions was measured in a falling ball viscometer described before (Lindemann and Rikmenspoel, 1972).

THE CONTRACTILE MODEL

In this section a brief description will be given of the model for ciliary contractility. The model will be introduced axiomaticly. An extensive explanation of the procedures that have led to its derivation has been given before (Rikmenspoel and Rudd, 1973).

In a sliding filament mechanism in an axoneme a dynein molecule produces an active moment m_e by forming a crossbridge to the adjacent tubulin fiber. As the tubulin fibers are attached only at the basal end, and are free to slide at the tip (Satir, 1965), the active moment produced by a crossbridge is apparent only at locations proximal to the crossbridge. At a point on the cilium at a distance s from the base, the total active moment is therefore the sum of the moments produced by the dynein crossbridges which are distal to s.

In a compound cilium, consisting of N axonemes at the basal region, the active moment M_{act} at s is thus:

$$M_{act}(s) = NDm_e \int_s^L f(\xi, t)\sigma(\xi)d\xi, \quad (1)$$

where D is the number of dyneins in one axoneme per unit length, L is the length of the cilium, and ξ is a running coordinate along the cilium. $f(\xi, t)$ denotes the fraction of dyneins which are attached as crossbridges at location ξ, at time t, and $\sigma(\xi)$ describes the tapering of the cilium towards the tip, normalized as $\sigma(o) = 1$.

Eq. 1 describes the simplest possible form of a sliding filament mechanism, with linear summing of the moments produced by the individual crossbridges. No assumptions are necessary to derive Eq. 1. A contractile model consists essentially of a prescription for the exitation $f(\xi, t)$, as a function of time and location on the cilium.

The tubulin fibers of an axoneme are able to slide relative to each other when the cilium is bent, except where adjacent fibers are bound together by crossbridges. When no crossbridges are attached the axonemes should be flexible (compare a stranded wire), the stiffness being only that of the matrix material and the membrane: ie_{mat}. If at a location s on the cilium crossbridges have formed, the tubulin fibers are not free to slide, and contribute to the stiffness. When a fraction $f(s,t)$ of the dyneins at s have formed crossbridges the extra stiffness at s is $ie_{\text{fibers}} f(s,t)$, where ie_{fibers} is the stiffness of an axoneme with all dyneins attached.

It was found necessary by Rikmenspoel and Rudd (1973) to average the stiffness as expressed above over a small length δs adjacent to s to avoid too abrupt changes in stiffness and to account for stretching of the fibers. For a compound cilium with N axonemes at the base, the stiffness $IE(s)$ at s thus becomes:

$$IE(s) = N[ie_{\text{mat}} + ie_{\text{fibers}} \int_{s}^{s+\delta s} f(\xi,t)\sigma(\xi)\mathrm{d}\xi \cdot (1/\delta s)]. \tag{2}$$

Eq. 1 and 2 show that the active moment and the stiffness vary over the cycle, dependent on the same excitation function $f(\xi,t)$. The sliding filament model gives a natural explanation for the intuitive notion that the cilium changes its stiffness during its cycle.

The motion of a model cilium as described above is computed with the equation of motion, in which the elastic moment M_{el} and the active moment M_{act} are balanced by the moment due to the viscous drag of the medium M_{visc}:

$$M_{\text{el}} + M_{\text{act}} = M_{\text{visc}} \tag{3}$$

The elastic moment is proportional to the curvature $\partial\theta/\partial s$ of the cilium at s, where θ is the angle made by the cilium with the line normal to the cell surface. It is convenient to use a dimensionless coordinate $z = s/L$ for the location on the cilium. The elastic moment M_{el} thus becomes:

$$M_{\text{el}}(z) = (N/L)ie(z)(\partial\theta/\partial z), \tag{4}$$

where $ie(z)$ is the stiffness of one axoneme, given as the expression in square brackets in Eq. 2.

In the same dimensionless coordinate the active moment M_{act} is:

$$M_{\text{act}}(z) = NLDm_e \int_{z}^{1} f(\xi,t)\sigma(\xi)\mathrm{d}\xi. \tag{5}$$

The viscous moment M_{visc} is proportional to the third power of the length L of the cilium:

$$M_{visc}(z) = kL^3M(\theta,z), \tag{6}$$

where k is the drag coefficient, given by Gray and Hancock (1955). The symbolic function $M(\theta,z)$ is a complicated algebraic expression in θ and z, the explicit form of which is given in Rikmenspoel and Rudd (1973).

The motion of a model cilium as defined in Eqs. 3–6 can be iterated in time as described in detail before (Rikmenspoel and Rudd, 1973). It is necessary before carrying out actual calculations to define the functions $\sigma(\xi)$ and $f(\xi,t)$ and to evaluate the constants occurring in Eqs. 2 and 4–6.

The shape function $\sigma(\xi)$ for the cylindrical cilia of *Paramecium* and *Opalina* is $\sigma(\xi) = 1$. For the cilium of *Mytilus* the shape measured by Baba and Hiramoto (1970) was approximated as $\sigma(\xi) = (1 - \xi)^{0.75}$. For *Phragmatopoma* the same shape function as for *Mytilus* was used, since no data on the shape were available.

This leaves the excitation function $f(\xi,t)$ to be defined. For the effective stroke of the cilia this function has been taken simply as $f_{eff}(\xi,t) = 1$. This represents an uniform and constant excitation of the dyneins at the side of the cilium that powers the effective stroke. In the transition phase between the effective stroke and the recovery stroke $f_{eff}(\xi,t)$ has to decay. The data for all cilia to be treated do not clearly show the period of this transition, however. The end of the effective stroke, and the transition to the recovery stroke will therefore not be further considered in this paper.

The recovery stroke is a more complicated phenomenon than the effective stroke. Distal to the sharp bend in the cilium during the recovery phase no active moment is present (Rikmenspoel and Rudd, 1973) and the cilium appears very flexible (Rikmenspoel and Sleigh, 1970). This has led to the proposal that the activation in the recovery stroke is caused by the sliding of the tubulin fibers relative to each other as the sharp bend passes the particular location in consideration. After the bend has passed, sliding no longer occurs, and the activation decays with a decay time τ_{rec}.

The different shapes of the cilium during the recovery stroke and the effective stroke necessitate a correction in the drag coefficient for the two phases. It was found (Rikmenspoel and Rudd, 1973) that this can be satisfactorily taken into account by taking the maximum value for $f_{rec}(\xi,t)$ to be 0.5.

If the time at which the bend of the recovery stroke starts to develop, is called t_o, and V is the velocity at which the bend progresses over the cilium, the activation at time t in the recovery stroke starts at a location $s_b = V(t - t_o)$ from the base. If the length of the bend section in which sliding occurs is called Δ, activation terminates at the point $V(t - t_o) - \Delta$ from the base. We thus find for the function $f_{rec}(\xi,t)$:

$$\begin{aligned}
f_{rec}(\xi,t) &= 0 \qquad L > \xi > V(t - t_o) \\
f_{rec}(\xi,t) &= 0.5 \qquad V(t - t_o) > \xi > V(t - t_o) - \Delta \\
f_{rec}(\xi,t) &= 0.5 \exp - \{t - t_o + [(\xi - \Delta)/V]\}/\tau_{rec} \\
&\qquad V(t - t_o) - \Delta > \xi > 0
\end{aligned} \tag{7}$$

With a value of τ_{rec} = 20 ms, the shape of the recovery stroke in a variety of cilia can be satisfactorily reproduced by the excitation function of Eq. 7 (Rikmenspoel and Rudd, 1973). Values for V, t_o and Δ have to be obtained in each case from the tracings of cilia, as explained below.

In the above the usual assumption is made that the effective stroke is powered by the dyneins on one side of the axonemes, and the recovery stroke by the dyneins on the other side. In the cases in which the effective stroke starts before the recovery phase has terminated, and the two overlap, the moments calculated with f_{rec}, respectively f_{eff} are added, having regard for the fact that they should carry opposite sign. The stiffnesses calculated with f_{rec} and f_{eff} are added, but since the stiffness is an inherently positive quantity, no sign reversal for the two phases is used. The additional inherent assumption, made in this, that the recovery and the effective stroke are two separate and independent phenomena, will be referred to again in the Discussion.

EVALUATION OF CONSTANTS

The model formulated above contains four constants which should be common for all cilia: m_e, D, ie_{mat}, and ie_{fibers}. The values for these quantities, derived previously (Rikmenspoel and Rudd, 1973) from an analysis of the motion of the cilium of *Sabellaria* are listed in Table I. The value of k, the viscous drag coefficient, was calculated for each of the cases to be treated from the formulae of Gray and Hancock (1955), as described previously (Rikmenspoel and Sleigh, 1970).

In the equation of motion (3) the elastic term M_{el} is in general one order of magnitude smaller than the active moment M_{act} and the viscous term M_{visc}. The latter two should therefore be roughly equal. Since the drag coefficient k can be expected to vary only weakly with the size of the cilia (Gray and Hancock, 1955; Rikmenspoel et al., 1960) a comparison of Eqs. 5 and 6 shows that NL should be proportional to L^3. For cilia of different size, N/L^2 should therefore be approximately constant.

Baba (1972) has published data for the diameter of *Mytilus* cilia with a length varying from 50 to 88 μm. If the diameter of these cilia, which is proportional to $\sqrt{N}$, is plotted against their length L, the result is indeed consistent with a linear relation. The axonemes in compound cilia are closely packed (Gibbons, 1961) with approximately 23 axonemes per μm^2 of cross section. The data of Baba (1972) can thus be normalized as:

$$N = 0.028L^2, \tag{8}$$

with L in microns. For a *Mytilus* cilium of L = 50 μm, Eq. 8 yields N = 70 axonemes.

The cilia of *Paramecium* have previously been considered as a single axoneme (Sleigh, 1962). However, in metachronal waves of *Paramecium* figured by Machemer (1974) it can be seen that where two cilia are implanted together their axonemes move together as a compound with N = 2. The cilia of *Opalina* are single axonemes, moving independently.

In *Phragmatopoma* axonemes are implanted in tight, narrow rows on the gill. Bundles of axonemes, which move as compound cilia, form a few micrometers from the

TABLE I

CHARACTERISTIC QUANTITIES FOR THE PRODUCTION OF ACTIVE MOMENTS AND STIFFNESS IN AN AXONEME

Quantity	Value
Moment produced by one dynein, m_e	1.5×10^{-13} dyn·cm
Density of dyneins on one side of axoneme, D	4.7×10^{6} dyneins/cm
Stiffness of matrix material, ie_{mat}	6×10^{-15} dyn·cm^2
Stiffness of fibers when crosslinked, ie_{fibers}	9.4×10^{-14} dyn·cm^2

base. Fig. 1 shows a scanning electron micrograph of the arrangement, in which the bundling is apparent. The length of the cilia in *Phragmatopoma* is rather uniform and varies with the size of the whole organism. For the experiments reported in this paper organisms were selected having cilia of a length $L = 25 \pm 2$ (SD) μm. From electron micrographs similar to that in Fig. 1 a value for the radius of the compound cilia of 0.55 μm was adopted, corresponding to $N = 22$ axonemes per compound. Table II summarizes the data for the length of the cilia from the above observations, and the number predicted from the scaling law of Eq. 8. The values for *Sabellaria* have also been inserted in Table II. It can be seen in Table II that the scaling law normalized to the data of Baba (1972) holds well for all species except *Opalina*. The cilia of *Opalina*, however, are very slow. The cycle frequency of 1–4 cps is typically five to six times

FIGURE 1 Scanning electron micrograph of a row of axonemes of *Phragmatopoma*. The bundling of axonemes into compound cilia can be clearly seen.

TABLE II

LENGTH, L, AND NUMBER OF AXONEMES OF CILIA OF VARIOUS ORGANISMS, INCLUDING NUMBER OF AXONEMES DERIVED FROM THE SCALING LAW OF EQ. 8

Organism	Length	Number of axonemes		Reference
		From scaling law	From data	
	μm			
Sabellaria	32	29	30	Rikmenspoel and Rudd (1973)
Paramecium	10	2.8	2	Machemer (1974)
Opalina	15	6	1	Tamm and Horridge (1970)
*Mytilus**	50	70	70	Baba (1972)
Phragmatopoma	25	18	22	This paper (Fig. 1)

* Used as normalization.

lower than that of the cilia of all other species in Table II. It appears therefore that this low frequency is due to the limited force the single axoneme in *Opalina* can generate. In the calculations to be reported below the number of axonemes has been taken as those from the "Data" column in Table II. For the cilia of *Mytilus*, in which the length varied, the number of axonemes was scaled according to Eq. 8.

PROCEDURE FOR CALCULATIONS

For all cilia calculations were started from a position at the beginning of the recovery stroke, to which was assigned $t = 0$. The progression of the bend in the recovery stroke proved in all cases treated here to accelerate towards the tip of the cilium. This is illustrated in Fig. 2 which represents a *Mytilus* cilium at 1.4 cPoise. The progression of the bend was approximated by a straight line, as indicated in Fig. 2, thus defining t_o and V of Eq. 7. A certain degree of freedom exists in drawing the straight line through

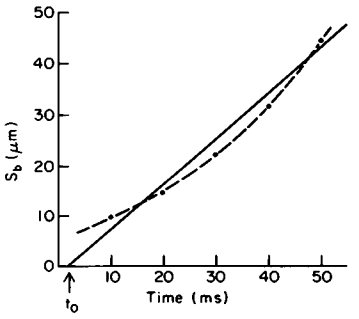

FIGURE 2 Progression of the bend during the recovery stroke in a cilium of *Mytilus* at 1.4 cP. s_b indicates the location at which the bend starts. The slope of the full line corresponds to the velocity of progression, V, used in the model calculations.

data points as in Fig. 2. In the actual calculations t_o and V were always adapted so that the aesthetically most pleasing motion of the model was obtained.

In the previous paper (Rikmenspoel and Rudd, 1973) computed ciliary motions were fitted to the observed ones by varying the number of axonemes of the model cilia. This was feasible because the exact number of axonemes was not known for the various organisms. In the present paper the number of axonemes is known in all cases to be treated, and all quantities of the model Eqs. 2, 4, 5, 6, and 7 are fixed. The fitting of the computed motions to the observed ones has been done by multiplying the functions $f_{\text{eff}}(\xi,t)$ and $f_{\text{rec}}(\xi,t)$ by an adjustable parameter, α_{eff} and α_{rec}, respectively. α_{eff} and α_{rec} essentially give the amount of activity of the model cilia normalized to that of *Sabellaria*, the organism from which all model quantities have been derived. The two parameters α_{eff} and α_{rec} will be referred to as the degree of activation of the cilia to be discussed below.

During the initial two-thirds of the recovery stroke the value of α_{rec} was adjusted so that the general computed motion was close to the observed one. At that value of α_{rec} the computations were then repeated, but with the stiffness as defined by Eq. 2 varied by factors of 2. The value for the stiffness in which the curvature in the bend of the computed cilium, averaged for the different positions, was closest to that for the observed cilium was adopted as the correct stiffness. The curvature of the bend in the recovery stroke is not very sensitive to the value of the stiffness (Rikmenspoel and Rudd, 1973). A variation in stiffness of a factor of 2 results roughly in a 20% change in curvature. The stiffness increase is therefore reported in round numbers for those cases where it applied.

The computations were then extended to the remainder of the ciliary cycle, and by trial and error the time t_{eff} at which the effective stroke started and the value of α_{eff} were determined. t_{eff} and α_{eff} were adjusted so that the best fitting spacing of the subsequent positions was obtained. For the effective stroke the stiffness was again varied as described above and that value was adopted that gave the closest fit for the maximum curvature of the cilium near the base during the effective stroke.

RESULTS

Paramecium

Fig. 3 (left) shows the motion of the *Paramecium* cilium as constructed from the data of Machemer (1972). Table III lists the pertinent quantities used in computing the best fitting model shown at the right side of Fig. 3. The stiffness during the recovery stroke was found to be that prescribed by the model, with no corrections necessary. During the effective stroke the model cilium has less curvature near the base than the data in the positions at 18 and 21 ms, but more in the positions at 24 and 27 ms for the uncorrected stiffness (Fig. 3, right). Since the data in Fig. 3 represent a constructed ciliary motion, not the tracing of one cilium through its cycle, the representation by the model is satisfactory, however. It appears that the stiffness generated by the model is approximately the correct one for *Paramecium*.

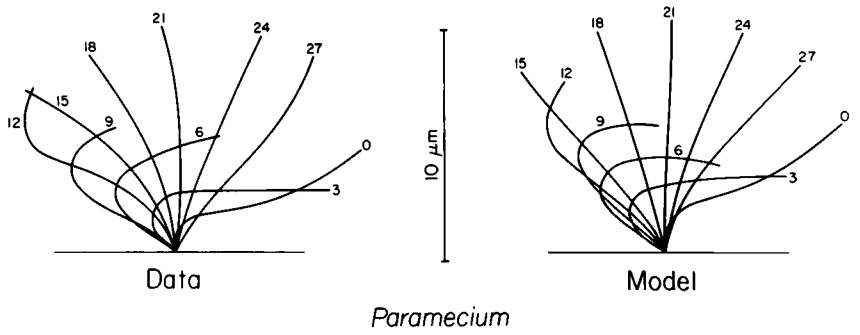

FIGURE 3 *Left*: Beat pattern of a cilium of *Paramecium*, constructed from the data of Machemer (1972). The numbers at the ciliary tip in this figure and in Figs. 4–8 denote the time in milliseconds. *Right:* Computed beat pattern of the model cilium.

It should be noted that the recovery stroke shown in Fig. 3 (left) is much faster (duration 12 ms) than the one diagrammed by Sleigh (1968) and analyzed before (Rikmenspoel and Rudd, 1973), which had a duration of 25 ms. The value for the activation α_{rec} found in the earlier analysis, which in the formulation of this paper would be $\alpha_{rec} = 0.65$, is therefore not in conflict with the value $\alpha_{rec} = 1.25$ presently reported.

Opalina

Fig. 4 (left) shows the tracing of the cilium of *Opalina*. The end of the effective stroke (beyond 225 ms in Fig. 4) is often slow and irregular, and it will not be considered here.

The recovery stroke of *Opalina* was reproduced as shown in Fig. 4 (right) with an activation $\alpha_{rec} = 1.2$. The stiffness, as generated by the model without corrections was found to give the correct maximum curvature in the bend in the cilium. During the effective stroke which starts at $t = 150$ ms, the cilium is *S*-shaped. In the model calculations, the motion of the tip of the cilium of approximately 0.15 μm/ms could be reproduced with an activation $\alpha_{eff} = 0.2$. In this case the shape of the cilium did not show an inflexion, but it remained singly curved. The inflexion and the rather sharp curvature near the base at 150 and 175 ms could be obtained by having a second "recovery" stroke, but with the active moment opposite in sign from the original one, starting at $t_o' = 125$ ms and progressing with a velocity $V' = 90$ μm/s. The activation of this

TABLE III

VALUES USED IN COMPUTING THE MOTION OF THE MODEL CILIUM OF *PARAMECIUM*

Quantity	Value
Length L (μm)	10
Number of axonemes N	2
Drag coefficient k (dyn· cm^{-2}·s)	0.0028
Activation recovery stroke α_{rec}	1.25
Activation effective stroke α_{eff}	1.25

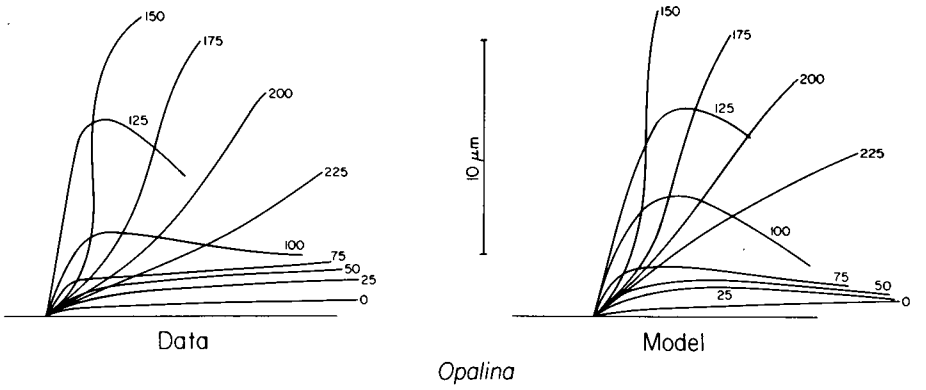

FIGURE 4 *Left:* Beat pattern of the cilium of *Opalina* (courtesy of M. A. Sleigh). *Right:* Computed beat pattern of the model cilium.

second recovery stroke was $\alpha'_{rec} = -0.2$. Fig. 4 (right) shows the effective stroke thus computed, using the normal stiffness for the model. The general shape of the effective stroke is fairly represented in the model, but the curvatures in the model cilium are too small, especially near the tip. At 225 ms the curvature in the model is actually reversed from that in the data. Reducing the stiffness improves the shape of the computed position at 150 ms, but produces inflexions at the positions at 200 and 225 ms.

It appears therefore that the general shape of the motion of the *Opalina* cilium can be explained with the model. It is doubtful that attempts to obtain a more precise fitting, which would require the introduction of *ad hoc* parameters, would lead to more insight.

The recovery stroke in cilia is started by the motion of the ciliary shaft at the base. The comparatively fast motion of the base in the period 125–150 ms during the effective stroke probably excites the second recovery stroke in *Opalina.*

The cilia of *Opalina* have been interpreted as an intermediate form of ciliary and flagellar beating patterns (Sleigh, 1968). Normal cilia show one effective and one recovery stroke. If *Opalina* with one effective and two recovery strokes is an intermediate between cilia and flagella, the logical extension would be that flagella have two effective and two recovery strokes. This proposal has indeed been made before (Rikmenspoel, 1971; Rikmenspoel and Rudd, 1973).

Table IV summarizes the values for the essential quantities adopted in producing the motion of the model *Opalina* shown in Fig. 4 (right).

Mytilus

Fig. 5 shows the motion of the *Mytilus* cilium at viscosities of 1.4, 3.4, 12, 26, 103, and 330 cP. Two different cilia at 1.4 cP are displayed to give an impression of the range of variation between cilia. The motion of the *Mytilus* cilia is not completely regular, and the variation between different cycles of the same cilium is of the same magnitude as that between the two cilia at 1.4 cP. In the latter part of the effective stroke the angu-

TABLE IV

VALUES USED IN COMPUTING THE MOTION OF THE MODEL CILIUM OF *OPALINA*

Quantity	Value
Length L (μm)	15
Number of axonemes N	1
Drag coefficient k (dyn · cm^{-2} · s)	0.0032
Recovery stroke	
Activation α_{rec}	1.2
t_o (ms)	40
V (μm/s)	160
Effective stroke	
Activation α_{eff}	0.2
Second recovery stroke	
Activation α'_{rec}	−0.2
t'_o (ms)	125
V' (μm/s)	90

lar velocity of the cilium is variable, with the cilium often coming to rest in an intermediate position (an "interkinetic pause," Sleigh, 1968). For this reason only the initial phase of the effective stroke is indicated, during which the motion is rather uniform.

It can be seen in Fig. 5 that the angle subtended by the ciliary stroke is reduced gradually from approximately 170° at 1.4 cP to approximately 10° at 330 cP. At 330 cP the motion in the effective stroke (beyond t = 1,000 ms) is slow and irregular. It is therefore not indicated in Fig. 5. At viscosities greater than 500 cP none of the cilia of *Mytilus* showed any motion.

Table V shows the length L, the number of axonemes N obtained from Eq. 8, and the calculated drag coefficient for the cilia in Fig. 5.

The recovery stroke of the model cilium could be reproduced for all cases of Fig. 5 without difficulty. Fig. 6 shows the motion computed for the model cilia at the various viscosities. As shown in Table V the activation α_{rec} necessary to produce the recovery strokes in Fig. 6 increased from around 1 at 1.4 cP to approximately 3 at 103 cP, after which it decreased. The increase of α_{rec} with viscosity indicates a mechanochemical feedback, analogous to the force-velocity relation in muscle. In view of the wide range of viscosities (200-fold) and of the duration of the recovery stroke (30-fold) the mechanochemical feedback is rather weak.

The stiffnesses which best fitted the curvatures in the bend during the recovery stroke was found to be slightly increased above that predicted by the model, except in the cilium at 1.4 cP A. The amount of increase, as Table V shows, tends to be larger at higher viscosities and for larger cilia.

The activation α_{eff} and its time of starting were adapted from the motion of the cilia to the left as described in the section Procedure for Calculations. The value for α_{eff}

TABLE V

EXPERIMENTAL AND MODEL QUANTITIES FOR THE CILIUM OF *MYTILUS* AT DIFFERENT VISCOSITIES

	Viscosity (cP)						
	1.4A	1.4B	3.4	12	26	103	330
Length L (μm)	48	48	72	50	50	44	32
Number of axonemes N	70	70	145	70	70	55	30
Drag coefficient k (dyn · cm^{-2} · s)	0.043	0.043	0.11	0.38	0.88	4.23	11.5
Recovery stroke							
Activation α_{rec}	1.28	0.79	0.83	1.87	2.42	2.91	1.67
Factor of stiffness increase	1	2	6	2	2	4	4
Effective stroke							
Activation α_{eff}	0.28	0.16	0.18	0.55	0.98	1.09	0.67
Start of activation (ms)	21	53	55	120	165	250	400
Factor of stiffness increase	100	200	600	200	200	400	—
Start of stiffness increase (ms)	28	53	105	135	165	325	—
Start of straightened cilium in data (ms)	30	55	105	135	165	330	—

was for all viscosities approximately a factor of 3 less than α_{rec} (Table V). The same, weak, mechanochemical feedback exists therefore for the effective as for the recovery stroke.

In all model cilia, after the recovery stroke had terminated, a very strong curvature developed. This could only be corrected by increasing the stiffness of the model cilia by a factor varying from 100 to 600 above the value predicted by the model. This sudden large increase in stiffness had to be applied from the time the cilium had a straight shape in the data. As shown in Table V this time does not coincide with the start of α_{eff} in most cases.

In the period after the recovery stroke in *Mytilus* has terminated and the cilia appear to be very stiff, the curvature as seen in Fig. 5 is slight, and often in the wrong direction to be interpreted as a bending resistance. It has therefore not been attempted to find a precise value for the stiffness. The values for the stiffness increase during the effective stroke in Table V are given in round numbers, and they carry a considerable uncertainty.

The model used to generate the actual, local stiffness of the cilia causes a step in its value distal to the bend in the recovery stroke. Typical values for the stiffness during the recovery strokes at 1.4 cP in Fig. 6 were 3×10^{-12} dyn·cm^2 near the base, and 5×10^{-13} dyn·cm^2 near the tip of the cilia. During the effective stroke at 1.4 cP the (increased) stiffness was typically 2–3 $\times$ 10^{-10} dyn · cm^2, near the base.

The small increase of the stiffness of the *Mytilus* cilium during the recovery phase, over the sum of the stiffnesses of the component axonemes can be easily explained by a small amount of friction between the axonemes. The fact that the increase appears correlated with the size (as at 3.4 cP) and with the occurrence of larger forces (at the higher viscosities) agrees well with the previous observation that in the very large and

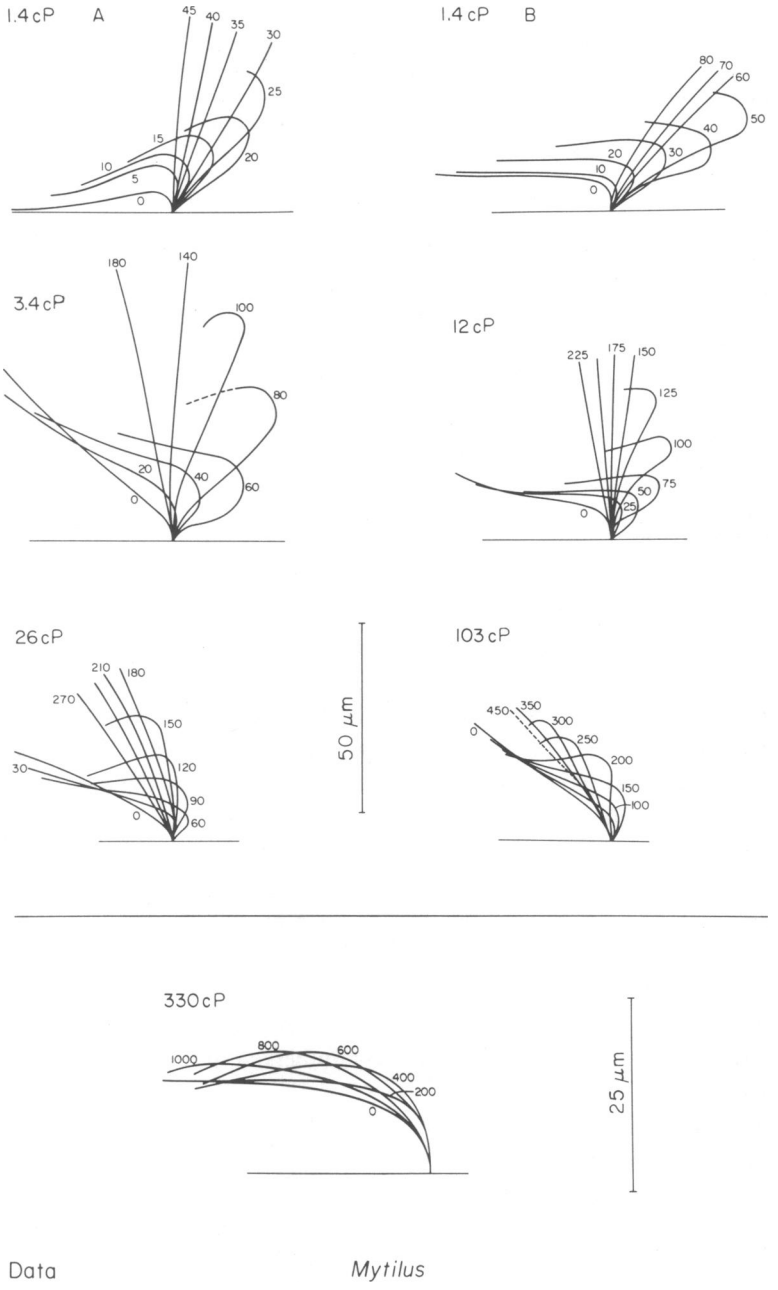

FIGURE 5 Beat patterns of cilia of *Mytilus* at various viscosities. Only the rather regular beginning phase of the effective stroke is shown. Dotted portions of positions indicate that the image of the cilium on the film was not completely clear. The cilium at 330 cP is shown at a different scale for clarity.

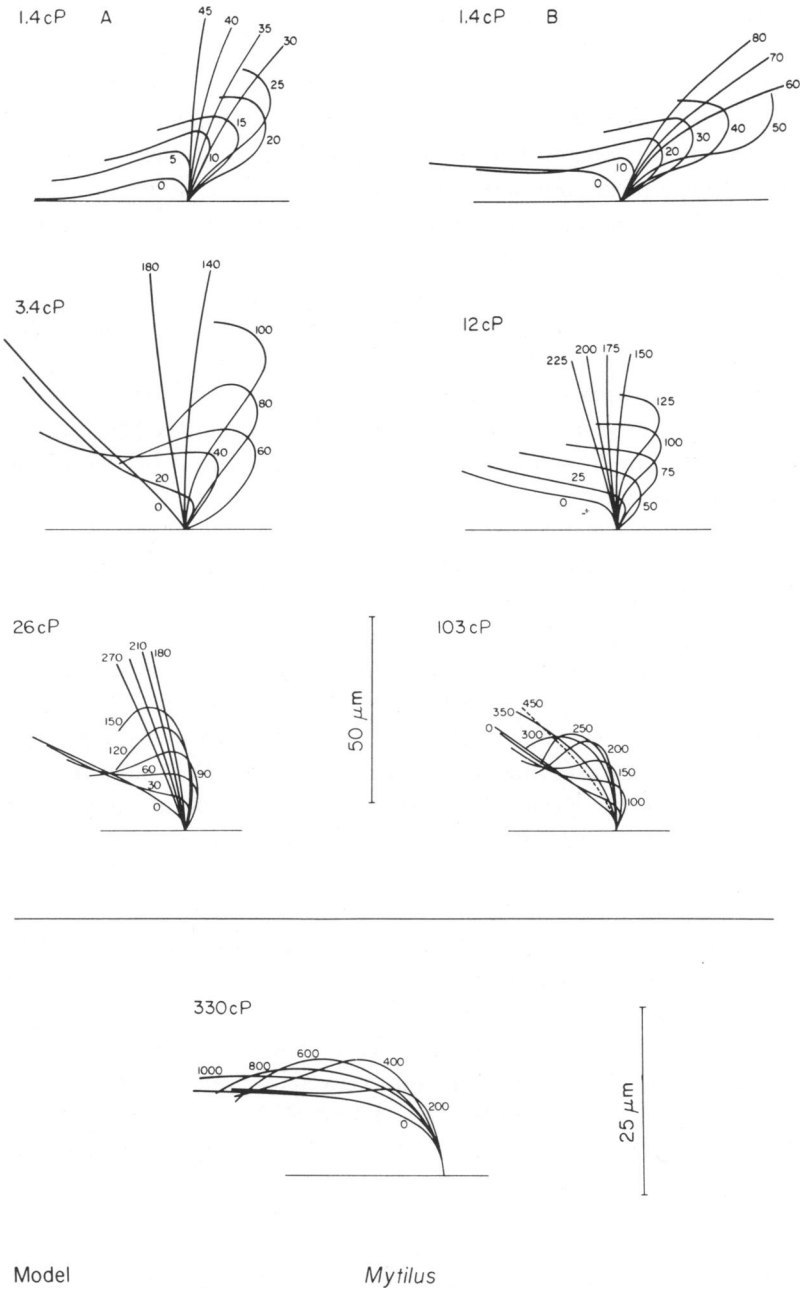

FIGURE 6 Computed beat patterns for the model *Mytilus* cilia at the different viscosities.

powerful combplates of *Pleurobrachia* a moderate amount of friction also occurs (Rikmenspoel and Rudd, 1973).

An axoneme of a *Mytilus* cilium at 1.4 cP has during the effective stroke, at an activation $\alpha_{eff} \approx 0.3$, a stiffness of $\approx 3.5 \times 10^{-14}$ dyn·cm^2 (compare Eq. 2). In a compound cilium with N axonemes solidly bound together, the stiffness would be proportional to the fourth power of the diameter, or to N^2. For a cilium of length $L = 50$ μm, with $N = 70$ axonemes bound together, the stiffness (with $\alpha_{eff} = 0.3$) would be $N^2 \times 3.5 \times 10^{-14}$ dyn·cm^2 $\approx 1.8 \times 10^{-10}$ dyn·cm^2. This is close to the value found above in the model calculations. It can be seen in Fig. 5 and Table V that in the period of the effective stroke in which the increased stiffness occurs the cilium undergoes almost no deformation, and therefore no motion of the axonemes relative to each other occurs. The cilium appears to behave in that phase as if the axonemes are tightly bound together or experience extremely heavy friction. This phenomenon is not caused by the Ficoll in the solutions at raised viscosity since it occurs also at 1.4 cP when no Ficoll is present.

The above mentioned values for the stiffness have to be compared with those reported by Baba (1972) which were typically 2–4 $\times 10^{-9}$ dyn·cm^2 for both the effective stroke and the recovery stroke in *Mytilus*. The analysis employed by Baba did not take into account the active contractile moments. Since the active moments are in general one order of magnitude larger than the elastic moments, the stiffness calculated while neglecting the former tends to come out 10 times too high. The *data* of Baba (1972) would in a complete analysis therefore give values for the stiffness in the effective stroke of *Mytilus* close to those reported in this paper. The values for the stiffness during the recovery stroke given by Baba (1972) are three to four orders of magnitude higher than those found presently. No explanation for this large discrepancy can be offered.

During the effective stroke the active contractile moment at the base of the model cilium of *Mytilus* at 1.4 cP was 3×10^{-8} dyn·cm (cilium A) and 1.7×10^{-8} dyn·cm (cilium B). Since during the effective stroke the curvature of the cilia is very small, the active moment is in spite of the high stiffness only slightly (20%) larger than the moment due to the viscous resistance of the fluid. The present model calculations are therefore in excellent agreement with the values given by Yoneda (1962) for the viscous moment of *Mytilus* cilia of 50 μm length at 1.4 cP of $(2 \pm 0.8) \times 10^{-8}$ dyn·cm (average and SD). It should be noted that the calculation of the viscous moment during the effective stroke is straight forward and requires no model assumptions.

Phragmatopoma

Fig. 7 shows the motion of the *Phragmatopoma* cilium at viscosities of 2.1, 3, 9, 30, 96, and 325 cP. It can be seen in Fig. 5 that up to a viscosity of 96 cP the form of the ciliary beat remains largely the same, and only at 325 cP is there indication of a narrowing of the beat pattern. At viscosities of 600 cP and higher no motion was observed in the cilia of *Phragmatopoma*.

The length of all cilia in Fig. 5 was close to 25 μm (Table VI). All model calculations

TABLE VI

EXPERIMENTAL AND MODEL QUANTITIES FOR THE CILIUM OF *PHRAGMATOPOMA* AT DIFFERENT VISCOSITIES

	Viscosity (cP)					
	2.1	3	9	30	96	325
Length L (μm)	22	23	22	27	27	26
Number of axonemes N	22	22	22	22	22	22
Drag coefficient k (dyn · cm^{-2} · s)	0.075	0.105	0.336	1.05	3.36	11.3
Recovery stroke						
Activation α_{rec}	0.52	0.50	0.91	3.7	8.3	12.2
Effective stroke						
Activation α_{eff}	0.78	0.74	1.0	4.0	5.4	4.9
Start of activation (ms)	55	82	110	160	187	379
Factor of stiffness increase	2	2	2	2	4	4
Start of stiffness increase (ms)	70	100	145	250	250	379

were performed for a fixed number of axonemes $N = 22$. It was judged that corrections for scaling according to Eq. 8 would not be meaningful within the small range of L.

The model representations of *Phragmatopoma* at the various viscosities are shown in Fig. 8. All recovery strokes were reproduced with a stiffness which is the sum of the normal stiffness of the axonemes. During the effective stroke the stiffness is slightly increased as shown in Table VI. As discussed above for the recovery stroke of *Mytilus* the increase of the stiffness with viscosity appears to point to a (small) friction between the axonemes. The effect is only marginally above what can be considered the confidence interval of this type of model calculations, however.

The activation increases more strongly with viscosity in *Phragmatopoma* than in *Mytilus*. As can be seen in Table VI, α_{rec} rises by a factor of 20 over the range of viscosities and α_{eff} by a factor of roughly 7. This points to a stronger mechanochemical feedback in *Phragmatopoma* than was found in *Mytilus*.

Even though the general shape of the cilia at the different viscosities is well reproduced by the model, a close inspection of Figs. 7 and 8 shows that the bend in the recovery stroke persists longer in the data than in the model. From a comparison with Table VI it can be seen that the model cilia start to straighten out as soon as the activation α_{eff} is started. In the data the recovery bend remains present, however, well into the effective stroke. As is related in the section Discussion, this may indicate that the way the elastic moments are calculated in the model is an oversimplification.

DISCUSSION

The general shape of a large variety of ciliary motions have been described successfully by the model in this paper and earlier (Rikmenspoel and Rudd, 1973). This leads one to expect that by simple variation of the activations for the recovery stroke, α_{rec}, and the effective stroke, α_{eff}, all variations of ciliary shapes will be obtainable with the

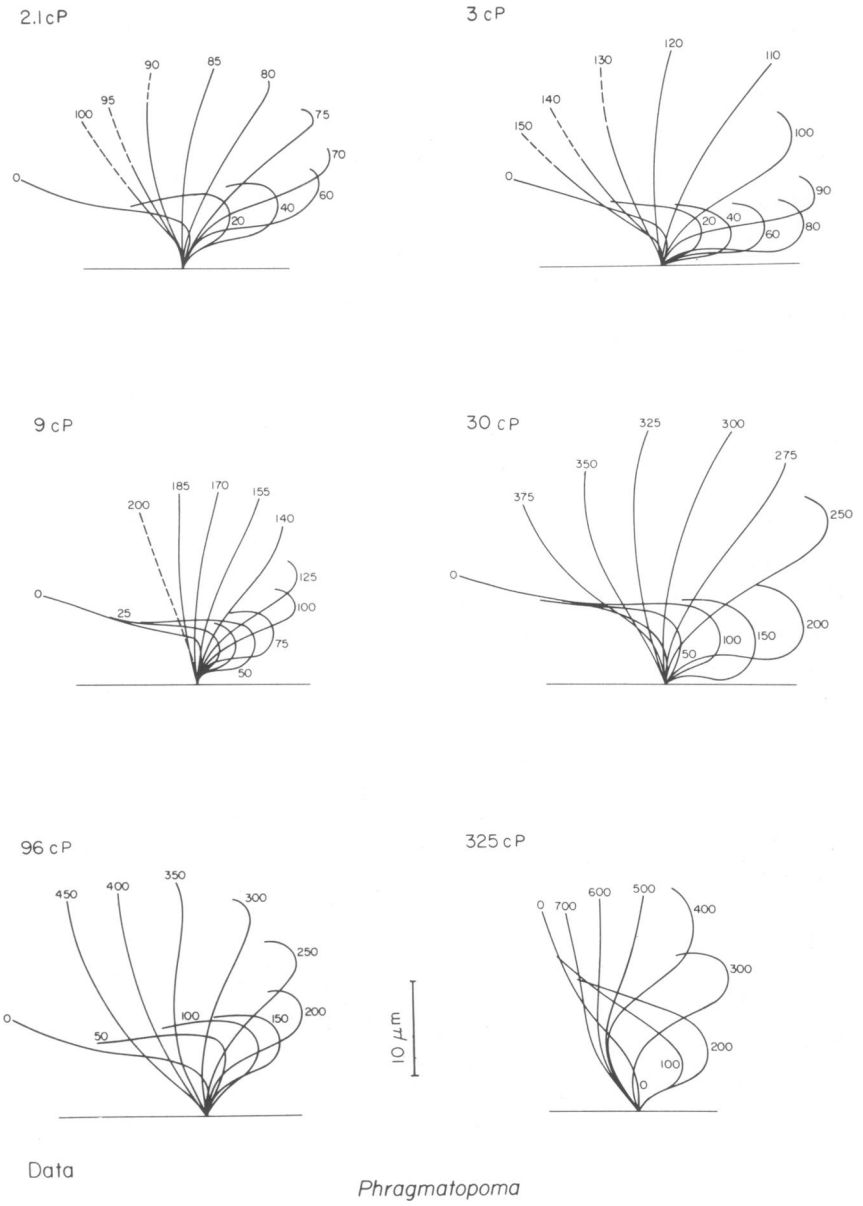

FIGURE 7 Beat patterns of cilia of *Phragmatopoma* at different viscosities. The direction of shear of the Nomarski optics used for illumination of the specimen was in the transition from the effective to the recovery stroke. This transition is therefore not displayed.

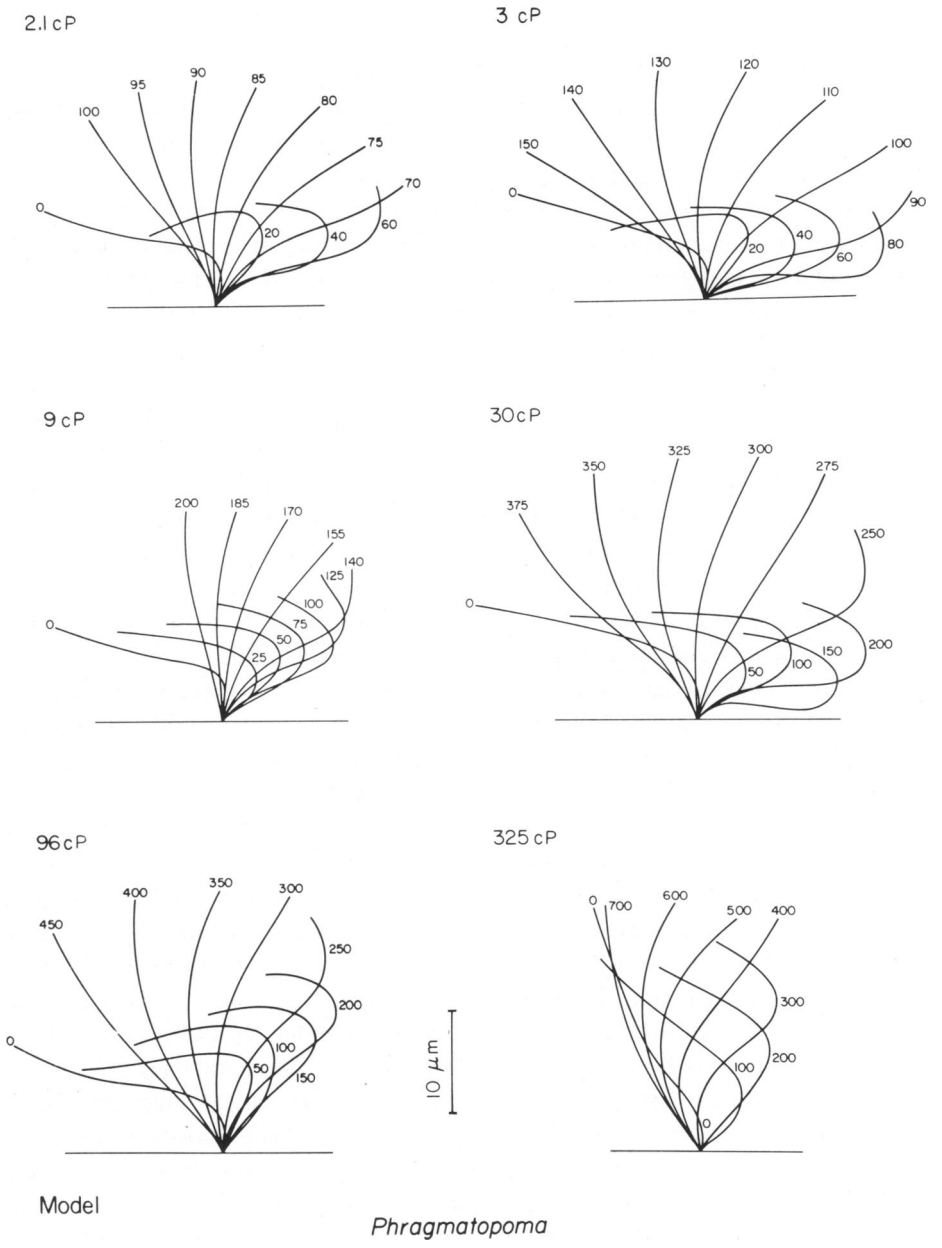

FIGURE 8 Computed beat patterns for the model cilium of *Phragmatopoma* at the different viscosities.

mechanisms used in the model to generate the active moments and the stiffness. Some of the limitations of the model are shown by the results in this paper which will be pointed out below.

The beat of the cilia of *Mytilus* and of *Phragmatopoma* is a planar, two-dimensional beat. This is shown by the observation that the cilia of both species remain in focus over their entire length throughout the cycle. The deviations out of the plane of focus are probably smaller than a micrometer in both cases.

In *Opalina* and in *Paramecium* the beat pattern is supposed to have a three-dimensional shape (Tamm and Horridge, 1969; Machemer, 1974). The tracings presented in Figs. 3 and 4 are therefore projections of the ciliary motion. In the photographs in Nomarski illumination published by Machemer (1972, 1974), the *Paramecium* cilia appear to be in focus over most of their length, indicating that the excursions perpendicular to the plane of beating are rather small.

Scanning electron microscopy (Tamm and Horridge, 1969) on *Opalina* has revealed that, in the recovery stroke, motions of the cilia of up to several micrometers occur perpendicular to the main plane of beating. Part of this may have been caused by preparative deformation. However, in earlier observations in light microscopy on living animals, Sleigh (1960) observed the ciliary beating of *Opalina* to be planar.

In general the projection of the motion in both *Paramecium* and *Opalina* is well represented by the model. This indicates that the two-dimensional model is adequate to describe the essentials of the contractile coordination in these cilia.

Details of the motion such as the relative spacing of various positions and the precise curvature of the proximal part during the recovery stroke are not well reproduced in the model cilia. It is most probable that better fits can only be obtained by introducing more complicated forms of the shape function $\sigma(\xi)$ of the cilia, and by introducing time and location variations of the activations α_{rec} and α_{eff}. As has been expressed above this would not add to the understanding of the phenomena, however.

In the transition period from recovery stroke to effective stroke in *Phragmatopoma* the bend in the model cilium is eliminated as soon as the activation for the effective stroke starts. This is caused by the stiffness generated by α_{eff} (compare Eq. 2). In the data of Fig. 7 it is clear that the bend in the real cilium remains. This is especially pronounced at 3, 30, 96, and 325 cP. It is quite possible that the cause of this effect is that the elastic moment M_{el} of Eq. 4, which tends to bring the cilium back to its equilibrium position, is not strictly proportional to the curvature. Eq. 4 presumes that the equilibrium position of the cilium is straight. If the equilibrium position, however, is that position which the cilium happens to have at the time the dynein crossbridges attach, the elastic moments would tend to maintain the shape, not to straighten it out. Since in general the ciliary shapes are rather well reproduced, it appears that the introduction of a variable equilibrium position would only serve as curve fitting in a few special positions. It has therefore not been attempted to introduce this extra complication.

In the model as formulated in this paper, the viscous resistance by the fluid sur-

rounding the cilia is represented by a drag coefficient, k, which is constant along the cilium. In recent years considerable advances have been made in analyzing the fluid motion around cilia (Blake and Sleigh, 1974; Brennen, 1974), which would make it possible to describe the fluid drag in more detail. The fact that the model is successful with the simplest hydrodynamic formulation (by means of a drag coefficient which does not vary with the location along the cilium) shows that there is no need for a more sophisticated treatment. This is also supported by the observation that the shape of the ciliary beat in *Sabellaria* (at a Reynolds number $R \ll 1$) is very similar to the shape of the beat in *Pleurobrachia* (in which $R \gg 1$), even though the hydrodynamics are quite different for these two species.

The present results appear to confirm the value for the stiffness of an axoneme at unit activation of 1×10^{-13} dyn·cm^2. Recently Lindemann (1975) has reported, from a new and different type of analysis, the stiffness of the sea urchin sperm axoneme as $(1.5 \pm 0.6) \times 10^{-13}$ dyn·cm^2, agreeing well with the above value. The anomalous, high stiffness of the *Mytilus* cilium in its straight positions remains a problem, though. It would be desirable to have an independent confirmation of what appears to be the binding together of the axonemes during the effective stroke in this compound cilium.

In *Paramecium* and in *Phragmatopoma* at 1.4 cP the activation is found close to 1, which would be expected in cilia with a normal beat pattern. It should be kept in mind that in fact the activation is normalized to that of *Sabellaria,* which has a ciliary beat very similar to that of *Paramecium* and *Phragmatopoma.* In *Opalina* the recovery stroke is the phase in which the transport of water is accomplished (Blake and Sleigh, 1974). In *Mytilus* the recovery stroke performs the essential function of the cilium, that of removing particles by a fast flicking action (Sleigh, 1962). In both these organisms the effective stroke represents a slow return of the cilium to the starting position. It is satisfying that for *Opalina* and *Mytilus* a normal activation, not very far from 1, is found for the recovery stroke, and a much lower activation (0.2–0.3) for the effective stroke.

The activation as a function of viscosity is plotted for *Phragmatopoma* and *Mytilus* in Fig. 9. In this figure it can be seen more clearly than in the Tables V and VI that up to approximately 100 cP in both organisms the activation increases in a rather regular fashion. The points at 325 cP for *Phragmatopoma* and at 330 cP for *Mytilus* should not be given great weight because the breakdown of the ciliary activity seems to start, according to Fig. 9, at around 100 cP, and the computed shapes for these high viscosities in Figs. 8 and 6, respectively, are not a very accurate fit to the observed ones. Up to 100 cP the curves for α_{rec} and α_{eff} in *Phragmatopoma* are approximately parallel with a slope of ≈ 0.7. The same holds for *Mytilus,* where the average slope is ≈ 0.45. Within the range of approximately 1–100 cP Fig. 9 seems to indicate that the mechanochemical feedback in the cilia of *Phragmatopoma* is different and stronger than that in *Mytilus.* However, Yoneda (1962) has reported that the moment developed by *Mytilus* cilia during the effective stroke increases ninefold with a viscosity rise from 1.4 to 33 cP. This indicates an almost identical mechanochemical feedback as presently found

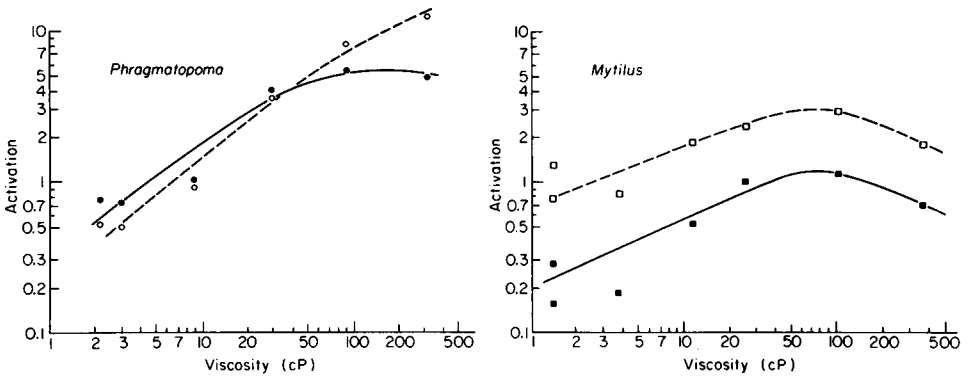

FIGURE 9 *Left:* Activation for the recovery stroke (open circles) and for the effective stroke (dots) of contractility in the cilia of *Phragmatopoma* as a function of viscosity. *Right:* Activation for the recovery stroke (open circles) and for the effective stroke (dots) of contractility in the cilia of *Mytilus* as a function of viscosity.

in *Phragmatopoma.* The variation of mechanochemical feedback in different samples of the same species is therefore probably of the same magnitude as the variation between species.

The fact that the activations α_{rec} and α_{eff} are found in many cases to be $\gg 1$, implies that the formulation of Eq. 1 in the section Contractile Model is not quite correct. The use of the actual density D of dynein molecules, as derived from electron microscopy, and an active moment m_e per dynein molecule should be replaced by the product $M_{sp} = Dm_e = 7.2 \times 10^{-7}$ dyn·cm/cm, which indicates the amount of active moment produced per centimeter axoneme length at unit activation. The high values for α_{rec} and α_{eff} at high viscosity indicate that at normal conditions only a fraction of the dynein crossbridges is actually attached, but that the active moment m_e per attached crossbridge is several times higher than the value 1.5×10^{-13} dyn·cm used.

In the paper in which the model was developed (Rikmenspoel and Rudd, 1973) it was found that the characteristic time for the crossbridge loosening is probably 5 ms, and the characteristic time of formation is of the order of 1 ms. This would cause a turnover of crossbridges during the various phases of the ciliary cycle. In complete analogy to the model developed by A. F. Huxley (1957) for striated muscle, the fraction of crossbridges actually attached at any given moment can be expected to increase as the ciliary cycle is slowed down, thus explaining the observed force-velocity relation. The data presently available do not seem sufficient, however, to attempt to quantitate the turnover and the attached fraction of crossbridges.

At normal viscosity the ratio of the activations for the effective stroke and the recovery stroke $\alpha_{eff}/\alpha_{rec}$ is 1.4 in *Phragmatopoma,* 1 in *Paramecium* and *Sabellaria,* and ≈ 0.2 in *Opalina* and *Mytilus.* This seems to confirm one of the basic premises of the model, that the mechanism in the effective stroke (simultaneous excitation of all dyneins at one side of the axoneme) is separate from that in the recovery stroke (excitation by sliding of the fibers in an axoneme relative to each other). The manner in

which the degree of activation in the recovery and in the effective model is brought about is presently unclear. In experiments by Eckert (1972) a reversal of the polarity of the ciliary beat was produced by electrical stimulation of the cell to which the cilia were attached. This clearly indicates the ability of the cell to prescribe the state of activation of the two mechanisms to the cilia.

The data in this paper illustrate some properties of cilia which are not model dependent. Figs. 5 and 7 show that as the viscosity increases ciliary motion slows down. For the effective stroke of *Mytilus* the motion can be characterized by the angular velocity ω. During the recovery stroke in *Mytilus* a point near the base (at s = 5 or 10 μm) executes a fast motion to the right in Fig. 5. As has been explained before (Rikmenspoel and Sleigh, 1970) the velocity of this motion can be expressed as an assigned frequency ν_{ass}. In *Phragmatopoma* the fraction of the cycle occupied by the recovery stroke remains approximately constant at all viscosities. For this species it is therefore sufficient to characterize the motion by the cycle frequency ν. In Fig. 10 are plotted as a function of the viscosity η the values for the quantities ω, ν_{ass}, and ν introduced above. The data show that all three characteristic frequencies decrease with $\eta^{-1/2}$. In Fig. 10 have also been plotted values for the angular velocity in the effective stroke of *Mytilus*, published by Yoneda (1962). Since Yoneda's data for ω were expressed in arbitrary units, they were normalized to the solid line in Fig. 10. The variation of angular velocity with viscosity in these earlier data is apparently the same as that found in the present experiments. Rikmenspoel et al. (1973) have shown that the frequency of the flagellar beat in bull sperm is also decreasing with $\eta^{-1/2}$. Brokaw (1972) has reported that in the sperm of *Ciona*, *Lytechinus*, and *Cheatopterus* the frequency of the

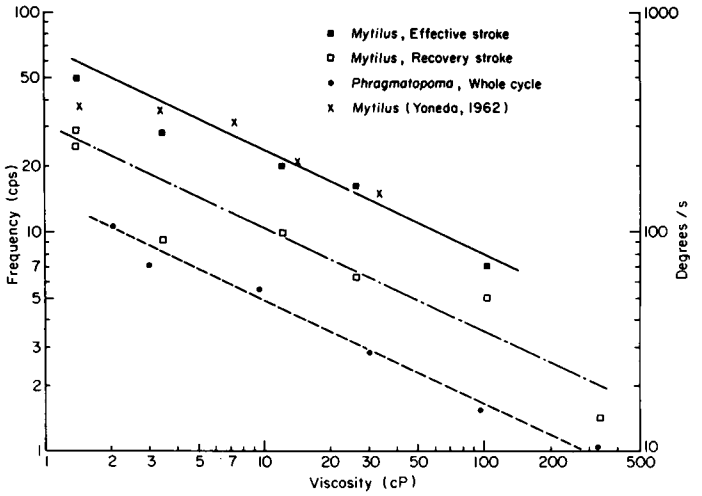

FIGURE 10 Angular velocity of the effective stroke and assigned frequency for the recovery stroke, both for the *Mytilus* cilium, and the frequency of the ciliary cycle for the *Phragmatopoma* cilium, as a function of viscosity. The data of Yoneda (1962) for the angular velocity in the effective stroke of *Mytilus* have also been inserted.

flagellar beat decreases with $\eta^{-1/4}$. When the data of Machemer (1972) are plotted on a double logarithmic scale, the frequency of the ciliary beat of *Paramecium* proves to decrease with $\eta^{-1/4}$. It is somewhat surprising to find an indication of two classes of a frequency-viscosity relation. Data over many more species will have to be taken, however, before it can be decided whether the slope of the frequency-viscosity relation varies rather widely and randomly with species, or whether distinctive classes exist.

In an earlier paper (Rikmenspoel, 1966) it was shown that small amplitude elastic theory applied to the case of sperm flagella predicts the wavelength of the motion in these structures to be dependent on one parameter C:

$$C = 2\pi k\nu L^4/IE. \tag{9}$$

The symbols in Eq. 9 all have the meaning adhered to in this paper: k = drag coefficient, ν = frequency, L = length, and IE = stiffness. It will be shown here that the parameter C of Eq. 9 evaluated for cilia suffices to obtain the velocity of propagation of the bend in the recovery stroke.

The value for ν to be used in Eq. 9 was taken as ν_{ass}, explained above. The stiffness IE represents the stiffness of the relaxed part of the cilium, where the propagation takes place, from the recovery bend to the tip: $IE = Nie_{mat}$. For the case of *Mytilus* the value of IE was increased with the appropriate factor for the recovery stroke in Table V. With the values of C thus obtained, the value of an "assigned wavelength"

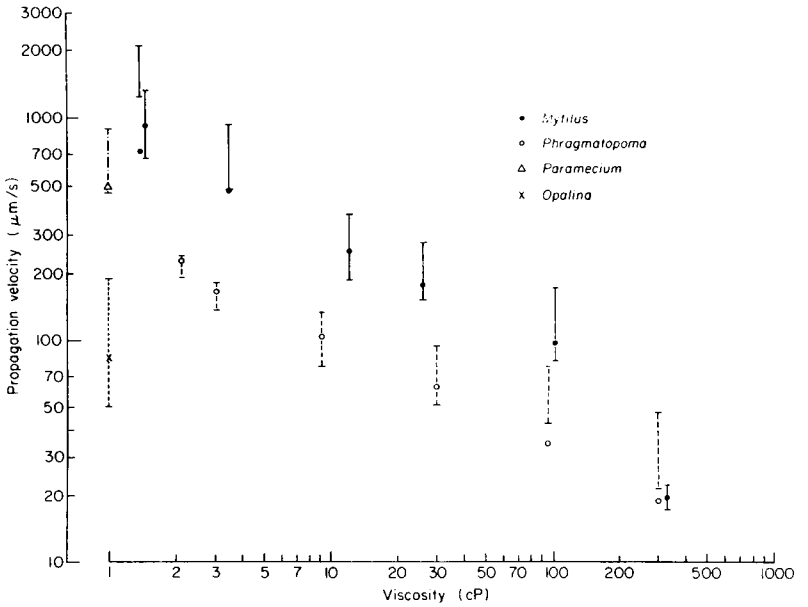

FIGURE 11 Velocity of propagation of the bend in the recovery stroke of various cilia, calculated by means of small amplitude elastic theory, under neglect of active contractile processes. The vertical bars show the range of the observed velocities as the bend travels along the cilium.

λ_{ass} can be read directly from Fig. 7 in Rikmenspoel (1966). The predicted value of the propagation velocity V is found as $V = \lambda_{ass} \nu_{ass}$.

Fig. 11 shows the calculated propagation velocity for all cilia in Figs. 3, 4, 5, and 7. The vertical bars in Fig. 11 show the observed velocities which, as illustrated in Fig. 2 above, vary as the recovery bend progresses. It can be seen from Fig. 11 that the extremely crude method of calculating, with neglect of all contractile processes, describes the propagation velocity quite well. This shows that the value of the propagating velocity cannot be used as a criterion to judge the validity of a contractile model.

My thanks are due to Mrs. Sandra Orris for taking the data on *Mytilus* and *Phragmatopoma* and for the scanning electron microscopy. The Dudley Observatory of the State University of New York at Albany is gladly acknowledged for making available the Stereoscan instrument. Mrs. Jacqueline Skolnik and Mr. Rick Schwartz have given the most valuable assistance with the running of the computer programs.

This investigation was supported in part by the National Institute for Child Health and Human Development through grant HD-6445, and by the National Institute of General Medicine through grant GM2014.

Received for publication 16 April 1975 and in revised form 18 July 1975.

REFERENCES

BABA, S. A. 1972. Flexural rigidity and elastic constant of cilia. *J. Exp. Biol.* **56**:459.

BABA, S. A., and Y. HIRAMOTO. 1970. A quantitative analysis of ciliary movement by means of high speed microcinematography. *J. Exp. Biol.* **52**:675.

BLAKE, J. R., and M. A. SLEIGH. 1974. Mechanics of ciliary locomotion. *Biol. Rev.* **49**:85.

BRENNEN, C. 1974. An oscillating boundary layer theory for ciliary propulsion. Abstracts of the Symposium on Swimming and Flying, Pasadena, Calif. 25.

BROKAW, C. J. 1972. Computer simulation of flagellar movement. II. Influence of external viscosity on movement of the sliding filament model. *J. Mechanochem. Cell Motility.* **1**:203.

ECKERT, R. 1972. Bioelectric control of ciliary activity. *Science (Wash. D.C.).* **176**:473.

EYKHOUT, P., and R. RIKMENSPOEL. 1960. High speed flash cinematography applied to studies of the movement of bull spermatozoa. *Res. Film.* **3**:304.

GIBBONS, I. R. 1961. The relation between the fine structure and direction of beat in gill cilia of a lamellibranch mollusc. *J. Biophys. Biochem. Cytol.* **11**:179.

GRAY, J., and G. J. HANCOCK. 1955. The propulsion of sea urchin spermatozoa. *J. Exp. Biol.* **32**:802.

HUXLEY, A. F. 1957. Muscle structure and theories of contraction. *Prog. Biophys. Biophys. Chem.* **7**:281.

KARNOVSKY, M. J. 1965. A formaldehyde-glutaraldehyde fixative of high osmolality for use in electron microscopy. *Am. Soc. Cell Biol. Annu. Meet. Abstr.* **5**:137*a*.

LINDEMANN, C. B. 1975. An analytical measurement of the stiffness of intact and demembranated sea urchin sperm during motility. *Biophys. J.* **19**(2, Pt. 2):160*a*. (Abstr.)

LINDEMANN, C. B., and R. RIKMENSPOEL. 1972. Simple viscometer for samples less than 1 ml. *J. Sci. Instrum.* **5**:178.

MACHEMER, H. 1972. Ciliary activity and the origin of metachrony in *Paramecium:* effects of increased viscosity. *J. Exp. Biol.* **57**:239.

MACHEMER, H. 1974. Ciliary activity and metachronism in protozoa. *In* Cilia and Flagella. M. A. Sleigh, editor. Academic Press, Inc., New York. 199.

RIKMENSPOEL, R. 1966. Elastic properties of the sea urchin sperm flagellum. *Biophys. J.* **6**:471.

RIKMENSPOEL, R. 1971. Contractile mechanisms in flagella. *Biophys. J.* **11**:446.

RIKMENSPOEL, R. 1974. Stiffness and moments in the cilium of *Mytilus* at raised viscosity. Abstracts of the Symposium on Swimming and Flying, Pasadena, Calif. 13.

RIKMENSPOEL, R., A. C. JACKLET, S. E. ORRIS, and C. B. LINDEMANN. 1973. Control of bull sperm motility. Effects of viscosity, KCN and thiourea. *J. Mechanochem. Cell Motility.* **2**:7.

RIKMENSPOEL, R., and W. G. RUDD. 1973. The contractile mechanism in cilia. *Biophys. J.* **13**:955.

RIKMENSPOEL, R., and M. A. SLEIGH. 1970. Bending moments and elastic constants in cilia. *J. Theor. Biol.* **28**:81.

RIKMENSPOEL, R., G. VAN HERPEN, and P. EYKHOUT. 1960. Cinematographic observations of the movements of bull sperm cells. *Phys. Med. Biol.* **5**:167.

SATIR, P. 1965. Studies in cilia. II. Examination of the distal region of the ciliary shaft and the role of the filaments in motility. *J. Cell Biol.* **26**:805.

SLEIGH, M. A. 1960. The form of beat in cilia of *Stentor* and *Opalina*. *J. Exp. Biol.* **37**:1.

SLEIGH, M. A. 1962. The Biology of Cilia and Flagella. Pergamon Press, New York.

SLEIGH, M. A. 1968. Patterns of ciliary beating. *In* Aspects of Cell Motility. P. L. Miller, editor. Academic Press, Inc., New York.

TAMM, S. L., and G. A. HORRIDGE. 1969. Critical point drying for scanning electron microscopic study of ciliary motion. *Science (Wash. D.C.).* **163**:817.

TAMM, S. L., and G. A. HORRIDGE. 1970. The relation between the orientation of the central fibers and the direction of beat in cilia of *Opalina*. *Proc R. Soc. Lond. Biol. Sci.* **175**:219.

YONEDA, M. 1962. Force exerted by a single cilium of *Mytilus edulis*. II. Free motion. *J. Exp. Biol.* **39**:307.